Available online at www.sciencedirect.com
SCIENCE DIRECT
Journal of Power Sources 153 (2006) 157–164
JOURNAL OF POWER SOURCES
www.elsevier.com/locate/jpowsour

Efficient sulfur-tolerant bimetallic catalysts for hydrogen generation from diesel fuel

Praveen K. Cheekatamarla *, Alan M. Lane

Department of Chemical Engineering, Box 870203, The University of Alabama, Tuscaloosa, AL 35487, USA

Received 2 March 2005; received in revised form 22 March 2005; accepted 22 March 2005
Available online 31 May 2005

Abstract

Catalytic autothermal reforming (ATR) of synthetic diesel and JP8 over supported metal catalysts has been investigated in the present study. Bimetallic catalysts exhibited superior performance compared to the commercial catalyst and the monometallic counterparts. BET, temperature-programmed desorption (TPD), temperature-programmed reduction (TPR) and XPS were utilized for characterizing these formulations, which showed that the enhanced stability is due to a strong metal–metal and metal–support interaction in the catalyst.

Keywords: Hydrogen; Fuel cells; Autothermal; Reforming; Diesel; Sulfur

1. Introduction

The reforming of higher hydrocarbons (e.g. gasoline or diesel) for fuel cell hydrogen is a challenging proposition not only because of sulfur problems but also because coking problems can be severe [1]. Therefore, the successful reforming of these fuels will largely depend on the development of a catalyst, which is resistant to both sulfur and coking. In order to avoid storing high-pressure hydrogen, the fuel can be generated in an onboard fuel processor [2,3]. For transportation applications, the primary focus is on reforming gasoline because the production and distribution infrastructure already exists [4,5]. For auxiliary power units, the focus is on reforming both gasoline (for automotive applications [6]) and diesel (for trucks and heavy-duty vehicles [7]). For portable power generation, the focus has been on reforming natural gas and liquified petroleum gas.

The conversion of hydrocarbon fuels to H_2 can be carried out by several catalytic reaction processes, including steam reforming (SR), partial oxidation (POX) and autothermal reforming (ATR). ATR involves the reaction of oxygen, steam and fuel to produce H_2 and CO_2. In essence, this process can be viewed as a combination of POX and SR and provides higher energy efficiency than the above processes [8].

The design of ATR catalysts can be challenging, particularly for gasoline/diesel reforming due to the complex and ill-defined nature of the fuel. ATR catalysts have to be active for both steam reforming and partial oxidation, be resistant to high temperatures and tolerant against sulfur poison and coke formation, especially in the catalytic zone with inadequate oxygen concentration.

Catalyst formulations for ATR fuel processors depend on the fuel choice and operating temperature. For methanol, Cu-based formulations can be used [9]. The catalysts based on the noble metals seem to be more active for the ATR reaction than the Ni-based ones [10,11]. Kikuchi et al. [12] studied the methane steam reforming reaction and they have demonstrated that the reactivity of different supported metals on SiO_2 follows this relative order: Ru, Rh > Ni > Ir > Pd, Pt > Co, Fe.

A method for developing a noble metal catalyst of improved resistance to sulfur compounds has been claimed [13]. The catalytic composition is obtained by subjecting the catalyst containing a noble metal from group VIII or a compound

* Corresponding author. Present address: Department of Chemical and Biological Engineering, Washington State University, Pullman, WA 99164, USA. Tel.: +1 303 949 1629; fax: +1 509 335 4806.
E-mail addresses: cheek004@bama.ua.edu (P.K. Cheekatamarla), alane@coe.eng.ua.edu (A.M. Lane).

0378-7753/$ – see front matter © 2005 Elsevier B.V. All rights reserved.
doi:10.1016/j.jpowsour.2005.03.176

thereof, a halogen and a carrier. For higher hydrocarbons, the catalyst typically comprises of metals such as Pt, Rh, Ru and Ni deposited or incorporated into carefully engineered oxide supports such as ceria-containing oxides [14].

Current interest in bimetallic catalysts is increasing, in particular because they show superior selectivity and resistance to poisoning as well as improved activity and stability. The main objective of the present work was to determine whether the autothermal reforming activity of Pt can be improved when a second metal is added to the substrate.

2. Experimental

2.1. Catalyst preparation

2.1.1. Ceria-based catalysts

The CeO_2 support material has a purity of 99.9%. The metal originates from a nitrate-based precursor material. Each catalyst was prepared by the incipient wetness method using distilled water as the solvent for the precursor materials. The catalysts were then dried in air at 110 °C overnight. Each catalyst was also calcined in air at 300–500 °C for 4 h. Bimetallic catalysts were prepared by depositing a metal first, drying, calcining and then depositing the second metal with subsequent drying and re-calcination. The overall concentration of the noble metal was maintained at a value of 1.25 wt.%

2.1.2. Alumina-based catalysts

The support material is Al_2O_3 (acidic, gamma). The active metal sites were obtained from nitrate precursors. The preparation technique adopted was incipient wetness method using distilled water as the solvent for the precursor materials. The catalyst was then dried in air at 110 °C overnight followed by calcination in air at 400 °C for 3 h. The catalyst was then reduced in a mixture of 5% H_2 and N_2 for 1 h at 350 °C. Bimetallic catalysts were prepared according to the procedure described above. The catalyst was then reduced in a mixture of 5% H_2 and N_2 for 1 h at 350 °C.

2.2. Reactor system

All the experiments were performed in a 3/8 in. adiabatic fixed-bed tubular (quartz) reactor. The synthetic diesel fuel (<10 ppm sulfur) and JP8 fuel (∼1000 ppm sulfur) were supplied by South West Research Institute (SWRI) and were not treated further. In case of a complex multi-component (>100) fuel like diesel, it is difficult to obtain a complete chemical breakdown. Conversely, from the elemental analysis (C: 83.92 wt.%, H: 14.66 wt.% and O: 1.42 wt.%) of the synthetic diesel, the average chemical composition of the experimental fuel was calculated. Liquid feed consisting of water and diesel was vaporized and mixed along with air in a pre-heater containing silicon carbide bed to enhance mixing. Calibrated HPLC pumps and unit mass flow controllers were used to control the flow rates. The gaseous mixture from the pre-heater was maintained at a temperature of 400 °C. The reactor with the catalyst bed was well insulated with 2 in. thick refractory ceramic fiber blanket to prevent heat loss and achieve the adiabatic reaction conditions. The hot-product gas leaving the reactor was cooled down in a heat exchanger/condenser system to separate water and liquid hydrocarbons from the product gas. Pressures above 2 psig were not encountered. The dry-product gas from the condenser was analyzed using a SRI gas chromatograph to monitor H_2, CO, CO_2, CH_4 and O_2 concentrations. In each test, 2 g of fresh non-diluted catalyst sample (pellets with an average size of 2 mm) was supported on a layer of quartz wool.

The experiments reported in this document were performed under the following conditions: H_2O/C ratio = 2.5, O_2/C ratio = 0.5, pre-heater/reactor temperature = 400 °C, gas hourly space velocity (GHSV) = 17,000 h^{-1}. These conditions were chosen according to our earlier work on synthetic diesel and JP8 fuel [15]. Oxygen was never observed in the effluent during any of the experiments at any of the temperatures tested. Condensate from the reactor was considered as unconverted/reformulated hydrocarbon. The carbon material balance from preliminary experiments showed about 14% loss, which can be attributed to unconverted hydrocarbon condensate, coke deposition on the catalytic surface and/or analytical error. Hydrogen yield defined in the experiments is the ratio of hydrogen in the products to that in the reactants (diesel + water). The measured temperature inside the reactor increased rapidly as the feed stream at 400 °C approach the surface of the catalytic bed and then gradually decreased from peak temperature of 800–365 °C down the catalytic bed, as noticed in our earlier work [15]. The average product composition at these reaction conditions was typically in the range of 55–60% H_2, 1–4% CO, 39–43% CO_2 and <1% CH_4 [15].

2.3. BET (surface area) and CO chemisorption (dispersion) measurements

BET surface area of the catalysts was analyzed by nitrogen adsorption–desorption technique. CO chemisorption at −80 °C was utilized to measure the dispersion of these catalysts using the pulse technique, this method is known to avoid to some extent the spillover phenomenon which affects accuracy of the data [16].

2.4. Temperature-programmed reduction (TPR) experiments

Temperature-programmed reduction was performed in a U-tube quartz reactor using a CHEMBET 3000 apparatus manufactured by Quantachrome, provided with thermal conductivity detector (TCD). Pellets (∼0.4 g) or fine powder (∼0.25 g) was used. To remove any water and CO_2 adsorbed on the surface, the catalysts were preheated to 250 °C for 2 h followed by purging and cooling in helium. Then, a reducing gas mixture consisting of 5% H_2 in helium was passed

through the catalyst and the temperature was ramped from 25 to 800 °C at a heating rate of 20 °C min^{-1}.

2.5. Temperature-programmed desorption (TPD) experiments

TPD of catalysts was carried out in the CHEMBET apparatus described above. In all the TPD experiments, the catalysts were preheated to 300 °C in helium for 1 h to remove residual H_2O and CO_2. After cooling down to room temperature in helium, the TPD data were acquired with a heating rate of 20 °C min^{-1} to 600 °C. The flow rate of the gas was typically 70 cm^3 min^{-1}.

2.6. XPS studies

XPS data were obtained using a Kratos Axis 165 with an Al anode as the X-ray source.

3. Results and discussion

The role of defect chemistry and the surface oxygen vacancies in determining the catalytic behavior of supported metal oxide systems is well known. The focus of this study was on the autothermal reforming activity of these catalysts as well as the effect and role of both the metal and the dopant on the catalytic properties. The experimental work involved developing, testing and characterizing: (a) single metal catalysts supported on reducible or non-reducible support and (b) bimetallic catalysts dispersed on these supports. Reactor studies involved the reforming of synthetic diesel fuel. Metal loadings generally range from 1 to 2% in the case of noble metals and 5–10% for non-noble metals.

3.1. Alumina-supported bimetallic catalysts

Three model catalysts were prepared to study the ATR activity of synthetic diesel fuel: Pt, Pd and Pt-Pd catalysts supported on alumina. Also, two different bimetallic catalysts were prepared by changing the order of impregnation: Pt(I)-Pd(II) and Pd(I)-Pt(II). The metal content and BET surface area of these catalysts is presented in Table 1. The surface area values evaluated from the nitrogen adsorption–desorption isotherms clearly indicate a decrease in the sorption capacity of the alumina support after Pt and/or Pd incorporation. As expected, the BET surface areas of the calcined catalysts were lower than that of the support and decreased further for the bimetallic catalysts.

Table 1
Chemical composition and surface area of Pd and/or Pt catalysts supported on alumina

Catalyst	Pt (Pd) (wt.%)	S.A. (m^2 g^{-1})
Alumina (A)	–	255
Pt/A	1.18	238
Pd/A	1.15	243
Pt-Pd/A	0.24 (0.90)	201
Pd-Pt/A	0.22 (0.90)	196

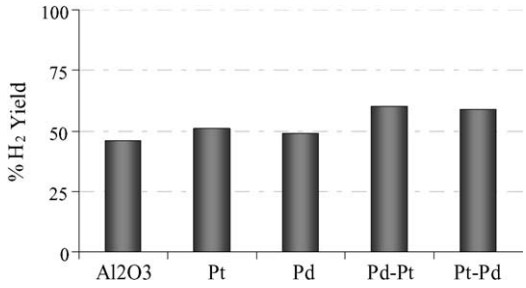

Fig. 1. Hydrogen yield during autothermal reforming of synthetic diesel fuel over alumina-supported Pd and/or Pt catalysts at $H_2O/O_2/C$ ratio of 2.5/0.5/1, reactor temperature of 400 °C and GHSV of 17,000 h^{-1}.

The autothermal reforming activity of these catalysts is shown in Fig. 1. Before carrying out the activity tests, all the catalysts were reduced at 350 °C in a 5% H_2/N_2 mixture. Catalysts loaded with Pt or Pd yielded about 50% hydrogen compared to 45% from bare alumina. The most interesting results are obtained from the bimetallic Pt-Pd catalysts. Each bimetallic catalyst showed high activity yielding ~60% hydrogen compared to 50% from their monometallic counterparts. The order of impregnation had no impact on the performance of these catalysts. The ATR activity on the Pt, Pd and Pt-Pd catalysts confirms a positive effect of Pt and Pd in the bimetallic catalyst because the level of activity of this system was higher than on either of the monometallic components in spite of fixed dispersion of the total active component.

Gaseous product distribution obtained after ATR of synthetic diesel fuel over alumina-supported Pd and/or Pt catalysts showed a decrease in the lower hydrocarbon (C_2–C_6) concentration by impregnating Pt or Pd on bare alumina. More dramatic results were obtained over the bimetallic catalysts yielding more hydrogen due to significant decrease in the lower hydrocarbon concentration coupled with improved CO oxidation activity resulting in lower concentration of undesired CO.

This higher intrinsic activity is probably due to the Pt–Pd interaction in the system. Temperature-programmed reduction studies and XPS analysis were carried out to understand this phenomenon.

TPR profiles of monometallic Pd (PdA), Pt (PtA) and the bimetallic (PtPdA) catalysts are shown in Fig. 2. TPR pattern of alumina carrier is not shown because of its non-reducible nature.

The TPR profile (Fig. 2) of the Pd catalyst shows a negative peak at 75 °C followed by a positive peak at 110 °C. The former can be assigned to desorption of hydrogen from the decomposition of a bulk palladium hydride formed through H-diffusion in to the Pd-crystallites [17], while the latter is attributed to the Pd oxide species. In contrast, the

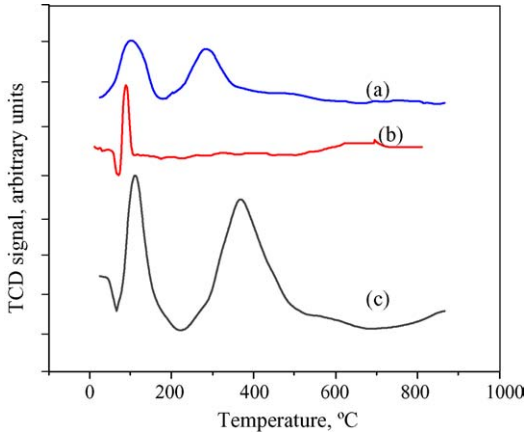

Fig. 2. Temperature-programmed reduction profiles for alumina-supported catalysts: (a) Pt (b) Pd and (c) Pt-Pd; operating conditions: 20 °C min^{-1}, 5% H_2 in He.

TPR profile of the Pt catalyst shows a broad reduction profile extending from 50 to 450 °C. All platinum oxide is reduced to Pt metal below 450 °C. Two reduction peaks, one at 100 °C and the other at 250 °C, were observed for Pt/Al_2O_3. The broadening suggests the presence of several Pt species with different oxidation states. These reduction peaks are slightly lower than the reported reduction temperature [18] probably due to differences in Pt content, calcination temperature, alumina type and temperature ramp rate during the TPR analysis.

The TPR profile of the bimetallic Pt-Pd catalyst is not simply the sum of the monometallic Pt and Pd catalysts. The bimetallic reduction profile exhibits peaks typical of PtO (100 °C) and PdO (110 °C) in addition to the Pd hydride decomposition peak at 75 °C, although both are much more intense than in the monometallic catalysts. Since the metal content is about the same in these catalysts, the increase in H_2 consumption associated with the metal oxide species seems to depend on the presence of second metal. In addition, the broader second peak centered at 400 °C detected in the Pt-Pd catalyst indicates the reduction of Pd species together with the co-impregnated Pt, probably due to some kind of interaction between the metals. Similar interactions in Pt-Pd systems were reported in TPR studies performed by Noronha [18]. These interactions between the metals leading to the formation of an active phase seem to be a probable reason behind the activity enhancement.

Significant differences were also observed in the XPS spectra of the Pt and/or Pd catalysts supported on alumina. A slight shift in the Pd $3d_{5/2}$ peak (~0.5 eV to higher binding energy) of the $Pt\text{-}Pd/Al_2O_3$ catalyst with respect to that of the Pd/Al_2O_3 catalyst was observed (not shown). The observed differences on the supported Pd and Pt-Pd surfaces may be due to the oxidation of Pd on the surface [19]. This positive shift may arise from changes in the electronic relaxation energy of Pd levels (220) in the presence of platinum, as suggested by Dufaux and Naccache [20].

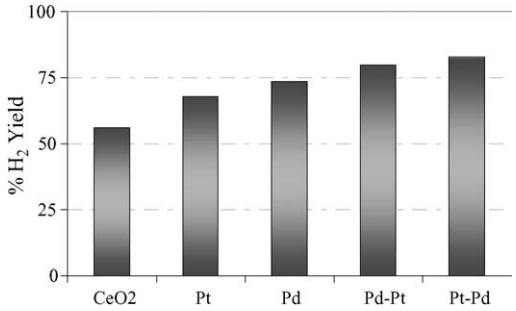

Fig. 3. Hydrogen yield during autothermal reforming of synthetic diesel fuel over ceria-supported Pt and/or Pd catalysts at $H_2O/O_2/C$ ratio of 2.5/0.5/1, reactor temperature of 400 °C and GHSV of 17,000 h^{-1}.

3.2. Ceria-supported bimetallic catalysts

As a part of fundamental study to identify the role of metals and metal oxides in autothermal reforming reactions, activity of bimetallic catalysts supported on a reducible ceria substrate was studied.

Three different metals viz. Pt, Pd and Ni were chosen for their ATR activity. These metals were chosen since it is generally accepted that Pt/Pd and Ni are the most preferred catalysts for oxidation and steam reforming, respectively. Hence, the presence of these active metals on the same support can facilitate heat transfer between exothermic oxidation and endothermic steam reforming at the micro scale, which allows advanced heat management and thermally efficient hydrogen production. The ceria-supported catalysts include monometallic components and their combinations with Pt: Pt (1.25 wt.%)-Ni (5 wt.%) and Pt (1 wt.%)-Pd (0.25 wt.%).

Two different bimetallic catalysts were also prepared by changing the order of impregnation on ceria substrate. It can be noted from Figs. 3 and 4 that all of these metals improved the ATR activity of ceria support. Similar to the results observed over the alumina-supported catalysts discussed in Section 3.1, the selectivity to produce hydrogen from diesel fuel was highest for the bimetallic catalysts compared to their monometallic counterparts. The impregnation order clearly had an effect on the activity in case of both bimetallic catalysts, as can be seen in Figs. 3 and 4.

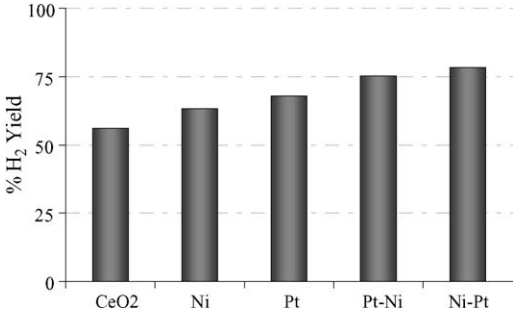

Fig. 4. Hydrogen yield during autothermal reforming of synthetic diesel fuel over ceria-supported Pt and/or Ni catalysts at $H_2O/O_2/C$ ratio of 2.5/0.5/1, reactor temperature of 400 °C and GHSV of 17,000 h^{-1}.

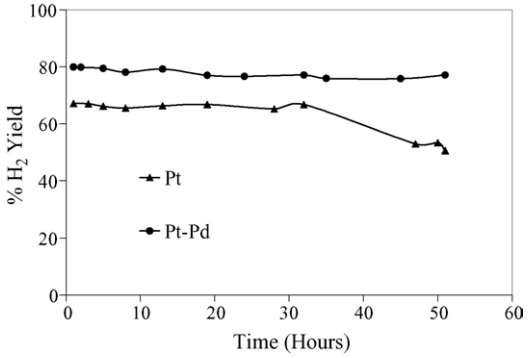

Fig. 5. Long-term activity of ceria-supported Pt and Pt-Pd bimetallic catalyst for the autothermal reforming of synthetic diesel fuel ~10 ppm S and JP8 ~1000 ppm S at $H_2O/O_2/C$ ratio of 2.5/0.5/1 and reactor temperature of 400 °C.

The higher level of activities observed over the bimetallic catalysts was further studied by introducing sulfur-containing feeds in to the ATR feed stream. This was achieved by testing the activity of these catalysts for reforming JP8 fuel. As shown in Figs. 5 and 6, significant loss in activity was observed over the Pt catalyst during ATR of JP8 fuel for more than 50 h. Similar experiments were carried out on the bimetallic catalysts and the results are presented in Figs. 5 and 6. The synthetic diesel is virtually sulfur-free whereas the JP8 has ~1000 ppmw S. It is clear from these plots that both the catalysts (Pt-Ni and Pt-Pd) exhibit resistance to sulfur poisoning in contrast to the activity decay observed over the monometallic Pt catalyst. Stable activity was observed over these catalysts even after testing them for more than 50 h in presence of significant amount of sulfur poison in the feed stream.

Higher intrinsic activity and sulfur tolerance of the bimetallic catalysts was further studied by conducting surface characterization studies in order to explain the phenomenon involved in the improved performance and the results are presented below.

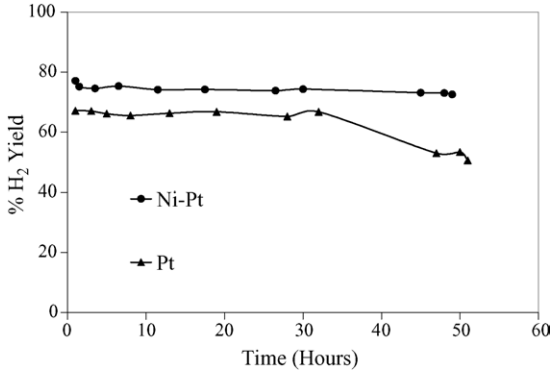

Fig. 6. Long-term activity of ceria-supported Pt and Pt-Ni bimetallic catalyst for the autothermal reforming of synthetic diesel fuel ~10 ppm S and JP8 ~1000 ppm S at $H_2O/O_2/C$ ratio of 2.5/0.5/1 and reactor temperature of 400 °C.

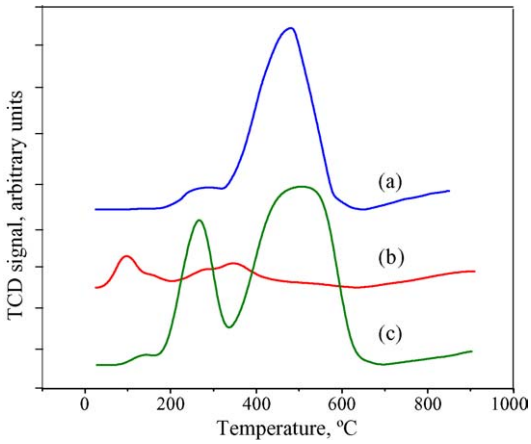

Fig. 7. Temperature-programmed reduction profiles for ceria-supported: (a) Ni (b) Pt and (c) Pt-Ni catalysts; operating conditions: 20 °C min^{-1}, 5% H_2 in He.

3.3. Characterization of Pt and/or Ni catalysts

The TPR data sets obtained from the ceria-supported Pt and/or Ni catalysts are portrayed in Fig. 7. The formation of two peaks centered at 250 and 450 °C in the Ni catalyst is due to the reduction of different oxidation states of supported nickel species in bulk-like phase [21].

The reduction peaks associated with the Pt catalyst are well documented in the previous section. The TPR spectrum obtained from the bimetallic Pt-Ni catalyst consists of three major features, one centered at 130 °C, one at 260 °C and the other at 500 °C. This profile is clearly a mixture of the two spectra above, excluding the new feature at 260 °C. The asymmetrical nature of the higher temperature feature suggests the existence of two reduction peaks, probably due to simultaneous reduction of Ni species and ceria support.

The peak at 260 °C due to the reduction of nickel oxide species seems to have enhanced in presence of Pt, suggesting that the structure and/or location of the NiO phase changes in the presence of Pt. One cannot definitively assign this state to the improved hydrogen yield over this catalyst relative to the other two, but does suggest that this is a strong possibility. The data suggests a possible scenario that may cause the resulting enhancement noted in the activity with the presence of both the Pt and Ni. A probable mechanism is that the Pt promotes reduction in adjacent Ni sites which adsorb O_2 and lend it to the CO or CH_x adsorption site, possibly Pt.

TPR data shows no lowering in the NiO reduction temperature after Pt incorporation onto Ni catalysts suggesting no Pt–Ni alloy formation. This can be anticipated considering that platinum has a larger atomic radius and lower surface tension than Ni. Also, the concentration of Ni is in excess (5%) compared to Pt (1.25%). As a result, Pt tends to be excluded out of the Ni matrix leading to a strong Pt isolation [22].

TPR spectra of the bimetallic Pt and Ni catalysts with different order of deposition on ceria support are shown in Fig. 8.

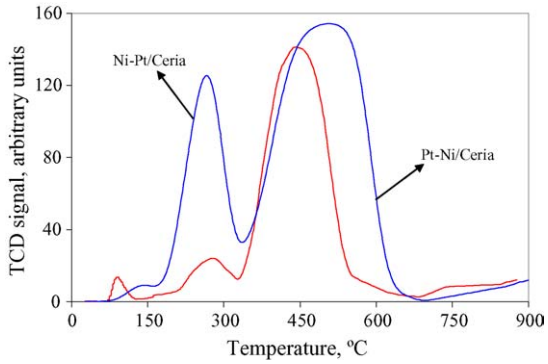

Fig. 8. Temperature-programmed reduction profiles for ceria-supported Pt-Ni and Ni-Pt catalysts; operating conditions: 20 °C min^{-1}, 5% H_2 in He.

Table 2
XPS characterization of Pt and Pt-Ni catalysts, Pt 4f and Ni 3s peak positions

Signal	Pt/C	Pt-Ni/C	Ni/C
Ni 3s	–	67.35	69.01
Pt $4f_{7/2}$	72.79	73.91	–
Pt $4f_{5/2}$	76.17	77.12	–

H_2 uptake over the Ni-Pt catalyst followed the same pattern as that of Pt-Ni catalyst (discussed above) except for the peak at 260 °C. This peak is due to the reduction of oxide species and is not as enhanced as that observed in the other catalyst, clearly demonstrating the fact that the order of deposition affects the oxidation states of metals. This difference in the reduction mechanism is also reflected in the ATR activity of these catalysts as noted in Fig. 4.

XPS characterization of the Pt and/or Ni catalysts was performed and Table 2 presents the results of the peak BE so analyzed. Assigned Pt peaks suggest 2+ and 4+ states of Pt. The BE of Pt 4f of Pt-Ni catalyst seems to be higher than that of Pt catalyst, while those of Ni 2p are similar between the bimetallic and the Ni catalyst (855.4–855.3 eV), as shown in Fig. 9.

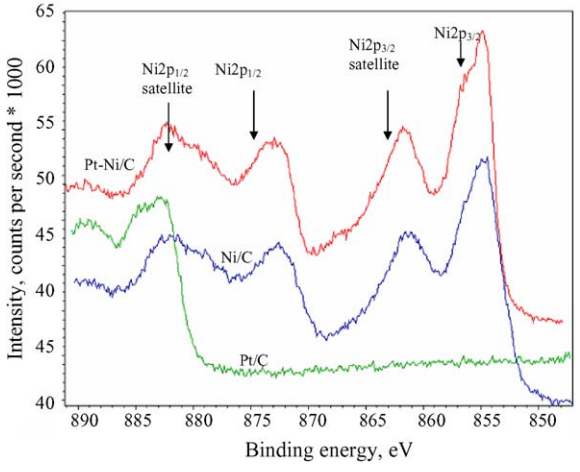

Fig. 9. XPS characterization of ceria-supported Pt and/or Ni catalysts: Ni 2p spectra.

In comparison with the ceria-supported Ni catalyst, the peak indicative of Ni 3s (Ni°) species in the bimetallic Pt-Ni catalyst is shifted towards a lower binding energy, indicating a higher electron density in the Ni species in the bimetallic catalyst. Although the Ni 2p BE values are comparable as described above, the Pt 4f BE value of the bimetallic catalyst is higher than that of the monometallic catalyst. This may contribute to the enhancement of activity and stability of the bimetallic catalysts. It can also be noted that, with platinum incorporation, the reducibility of the Ni species increased as observed in the TPR experiments.

The ceria-supported Pt-Ni catalysts are even more active and stronger against deactivation in autothermal reforming of diesel fuel than the corresponding monometallic Ni and Pt catalysts. The activity of these catalysts seems to depend on the order of metal loading and the formation of different oxidation states during the synthesis of the catalysts. XPS and TPR data indicate that the amounts of exposed Ni and Pt sites are different among the catalysts, corresponding with the differences in the catalytic activity and stability.

3.4. Characterization of Pt and/or Pd catalysts

The H_2-TPR profile of the unreduced bimetallic Pd-Pt catalyst showed marked differences to those of the monometallic catalysts. A sharp peak at about 100 °C is observed, which is more intense than that in the monometallic Pd catalyst, perhaps pointing to the formation of distinct PdO species, so leading to a small reduction in temperature and a much greater quantity of this species. These species alone cannot be attributed to the improved activity and selectivity of the bimetallic catalysts. Since the influence of bimetallic dispersion is not well understood during the TPR experiments, further analysis was carried out by XPS characterization and H_2 chemisorption.

Fig. 10 presents the TPD profile of H_2 from the ceria-supported Pt and/or Pd catalysts obtained following H_2 adsorption at 25 °C. Four major peaks at 120, 190, 310 and 680 °C can be distinguished on the Pt/ceria catalyst after H_2 chemisorption at 25 °C. For the bimetallic Pt-Pd/ceria

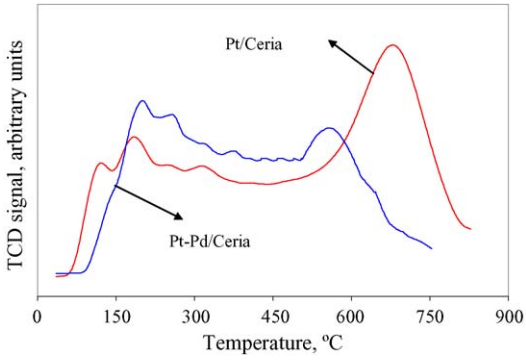

Fig. 10. Temperature-programmed desorption profile of H_2 obtained over Pt/ceria and Pt-Pd/ceria after H_2 adsorption at 25 °C; operating conditions: 20 °C min^{-1} to 600 °C.

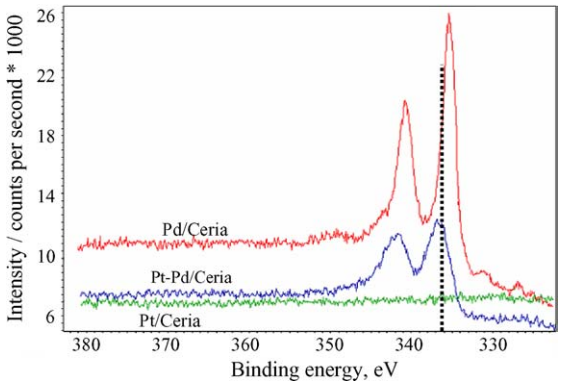

Fig. 11. XPS characterization, Pd 3d core level spectra of ceria-supported Pt and/or Pd catalyst samples.

catalyst, significant differences can be observed in the desorption profile. While the first three peaks at 160, 200 and 360 °C may correspond to the respective three peaks on the Pt/ceria, the peak at 680 °C has shifted to a lower temperature (560 °C).

In addition to the shift in the high-temperature peak, the amount of hydrogen desorption decreased substantially over the bimetallic catalyst. This may correspond to the strongly bound H species in case of the monometallic catalyst, probably the hydride or the hydrogen species in the subsurface layers of the metal catalyst [23]. While the major hydrogen species desorb at temperatures below 360 °C from the bimetallic catalyst, they remain on Pt/ceria surface at temperatures higher than 400 °C. The H–metal bond on the Pt/ceria catalyst appears to be stronger than that on the Pt-Pd/ceria, suggesting that an interaction between Pt and Pd leads to weakening of H–metal bond and, hence, better ATR activity compared to its monometallic counterparts.

The Pd 3d core level spectra for Pt-ceria, Pd-ceria and Pt/Pd-ceria catalysts studied are shown in Fig. 11. For the monometallic Pd catalyst, the binding energy of the Pd $3d_{5/2}$ level emerged at 335.4 eV and was assigned to PdO [16]. For the bimetallic Pt-Pd catalyst, a decrease in the Pd $3d_{5/2}$ signal in addition to a positive binding energy shift to 336.5 eV was found.

The positive shift possibly arises from changes in the electronic energy levels of Pd (2 2 0) in the presence of a second metal [16]. This close Pt-Pd contact may account for the observed decrease in the surface exposure of Pd due to the dilution effect of Pt on the bimetallic interaction.

However, the decrease in the surface coverage of Pd indicates some Pt surface isolation in the bimetallic particles, which could lead to secluded Pt cluster on the Pd surface. Isolation of Pd in silica–alumina-supported Pt-Pd particles was also found by Rades et al. [24]. These results clearly indicate that the catalytic behavior of Pt-Pd/ceria for the ATR of sulfur laden fuels is closely related to the presence of isolated Pt species, in addition to the weak metal–hydrogen bond strengths in the bimetallic catalysts, as observed in the H_2-TPD studies.

These kinds of species are claimed to be responsible for the high-sulfur tolerance of supported bimetallic catalysts [25,26]. Consequently, the enhanced performance of the Pt-Pd catalysts may be attributed to the presence of a bimetallic interaction, which reduces the tendency of Pt/Pd to chemisorb sulfur or form bulk sulfide and subsequent spillover on to the ceria support.

4. Conclusions

Catalytic autothermal reforming of synthetic diesel and JP8 fuel was investigated for fuel cell hydrogen. Experimental results revealed that the impregnation of Ni or Pd (in addition to Pt) on alumina or ceria not only improves the activity but also modifies the catalyst to resist poisoning from sulfur present in the feed. Characterization of these formulations showed that the enhanced stability is due to a strong metal–metal and metal–support interaction in the catalyst. The improved performance of the bimetallic catalysts is due to structural and electronic effects rather than the degree of metal dispersion.

Acknowledgements

This project was supported by Argonne National Laboratory. Helpful discussions with Dr. Theodore Krause are gratefully acknowledged.

References

[1] G.K. Acres, J. Power Sources 100 (2001) 60.
[2] H.L. MacLean, L.B. Lave, Prog. Energy Combust. Sci. 29 (2003) 1.
[3] T.R. Ralph, G.A. Hards, Chem. Ind. 69 (1998) 337.
[4] M.W. Melaina, Int. J. Hydrogen Energy 28 (2003) 743.
[5] R.L. Espino, J.L. Robbins, Proceedings of 30th International Symposium on Automotive Technology and Automation, 1997, p. 16.
[6] Delphi Automotive Systems, News release, October 2003, http://www.delphi.com/news/pressReleases/pr439-02162001.
[7] M.H. Ronald, J.F. Robert, Appl. Catal. A: Gen. 221 (2001) 443.
[8] S. Wieland, F. Baumann, K.A. Startz, Proceedings of the Fuel Cell Seminar on New Catalysts for Autothermal Reforming of Gasoline and Water-Gas Shift Reaction, 2000, p. 225.
[9] S. Marino, P. Bellview, K. Casson, Appl. Catal. B: Environ. 66 (1994) 33.
[10] A.T. Ashcroft, A.K. Cheetham, J.S. Foord, M.L.H. Green, Nature 344 (1990) 319.
[11] P.D.F. Vernon, M.L.H. Green, A.K. Cheetham, A.T. Ashcroft, Catal. Lett. 77 (1990) 181.
[12] E. Kikuchi, S. Tanaka, Y. Yamazaki, Y. Morita, Bull. Jpn. Petro. Inst. 16 (1974) 95.
[13] Process for manufacturing a group VIII noble metal catalyst of improved resistance to sulfur, and its use for hydrogenating aromatic hydrocarbons, US Patent 4,225,461.
[14] I.W. Carpenter, J.W. Hayes, US Patent 2,325,506, 1999.
[15] P.K. Cheekatamarla, A.M. Lane, J. Power Sources 152 (2005) 256–263.
[16] B. Andersson, D. Duprez, Appl. Catal. B: Environ. 22 (1999) 215.

[17] H. Lieske, J. Catal. 81 (1983) 17.
[18] F.B. Noronha, Appl. Catal. 78 (1991) 125.
[19] R.E. Cavicchi, M.J. Tarlov, S. Semancik, Surf. Sci. 257 (1991) 70.
[20] M. Dufaux, C. Naccache, J. Chem. Soc., Faraday Trans. 74 (1978) 440.
[21] Z. Paal, G. Menon, Catal. Rev. Sci. Eng. 25 (1983) 229.
[22] K. Otto, J.E. Vries, Appl. Catal. B: Environ. 1 (1992) 1.
[23] J.L. Rousset, B. Tardy, J.C. Bertolini, J. Catal. 149 (1994) 404.
[24] T. Rades, J.K. Lee, H.K. Rhee, Catal. Let. 29 (1991) 91.
[25] W.H. Sachtler, A. Stakheev, Catal. Today 12 (1992) 283.
[26] S.T. Homeyer, W.H. Sachtler, Stud. Surf. Sci. Catal. 49 (1989) 975.